AD NUMBER
AD904040
NEW LIMITATION CHANGE
TO **Approved for public release, distribution unlimited**
FROM **Distribution authorized to U.S. Gov't. agencies only; Test and Evaluation; SEP 1972. Other requests shall be referred to Naval Weapons Lab., Dahlgren, VA 22448.**
AUTHORITY
NWL ltr 16 Aug 1973

DISCLAIMER NOTICE

THIS DOCUMENT IS BEST QUALITY PRACTICABLE. THE COPY FURNISHED TO DTIC CONTAINED A SIGNIFICANT NUMBER OF PAGES WHICH DO NOT REPRODUCE LEGIBLY.

NWL TECHNICAL REPORT TR-2794
September 1972

FINITE DIFFERENCE CALCULATIONS OF THE FREE-AIR GUN BLAST ABOUT THE MUZZLE OF A 5"/54 NAVAL GUN

by

Dr. G. R. Moore

Test and Evaluation Department

FOREWORD

This document presents the calculations of a 5"/54 Naval gun free-air gun blast using a two-dimensional finite difference hydrodynamic code. This work was performed under the Naval Weapons Laboratory independent research/independent exploratory development program.

This report has been reviewed by D. C. Ross and F. F. Churchill of the Test and Evaluation Department.

Released by:

J. H. MILLS, JR.
Head, Test and Evaluation Department

ABSTRACT

A two-dimensional hydrodynamic code has been used to calculate the free-air blast field about the muzzle of a 5"/54 Naval gun. The calculated blast pressure wave as a function of time is presented along with the velocity field. Calculated overpressures and durations are compared with experimental data. The calculations predict the formation and location of the shock bottle and formation of the "smoke ring".

CONTENTS

INTRODUCTION

The phenomena associated with the free-air blast created by the releasing of hot gases as a projectile leaves the muzzle of a gun has been of interest for some time. Many experimental investigations [for example, references (1) and (2)] have been undertaken to determine the free-air blast parameters such as overpressure or impulse. These investigations have led to several empirical formulas for the free-air overpressure field [references (3) and (4)] about the muzzle of a gun. These investigations have primarily been done using pressure transducers, from which the free-air blast parameters of overpressure, positive duration, impulse and arrival time of the shock front can be determined at various positions about the gun muzzle. These investigations have shown that the free-air blast field is two-dimensional, that is, symmetical about the barrel axis.

Several hydrodynamic codes have in recent years been developed for the solution of one and two dimensional hydrodynamic problems. These codes numerically integrate the hydrodynamic equations of motion, which constitute a set of nonlinear partial differential equations. These codes have been used to investigate the hydrodynamics of such problems as spherical charges, shaped charges and supersonic flows. The objective of this report is to show that a two dimensional hydrodynamic code may be used to calculate the free-air blast field about the muzzle of a gun. Calculations on a 5"/54 Naval gun have been carried out and are compared with experimental data.

The hydrodynamic code used for the calculations presented in this report was the one-material SHELL code. The SHELL family of hydrodynamic codes uses the Eulerian form of the equations of motion which considers the mass in the grid system to be a continuum rather than discrete particles. Numerous blast-wave calculations have been performed using the SHELL codes such as those presented in references (5) through (8). The SHELL code used in the calculations presented here was obtained from the Air Force Weapons Laboratory, Kirtland AFB, New Mexico.

EQUATIONS OF MOTION

The hydrodynamic code used, SHELLTC, is a one material, two-dimensional, pure Eulerian code. The free-air blast about the muzzle of a gun is cylindrically symmetric about the barrel axis and thus two-dimensional. The hydrodynamic equations of motion for axisymmetric, inviscid compressible flow are given by:

Conservation of Mass

$$\frac{\partial \rho}{\partial t} + \frac{\partial (r \rho u)}{\partial r} + \frac{\partial (\rho v)}{\partial z} = 0 \tag{1}$$

Conservation of Momentrum - r direction

$$\rho \left(\frac{\partial u}{\partial t} + u \frac{\partial u}{\partial r} + v \frac{\partial u}{\partial z} \right) + \frac{\partial p}{\partial r} = 0 \tag{2}$$

Conservation of Momentrum - z direction

$$\rho \left(\frac{\partial v}{\partial t} + u \frac{\partial v}{\partial r} + v \frac{\partial v}{\partial z} \right) + \frac{\partial p}{\partial z} = 0 \tag{3}$$

Conservation of Energy

$$\rho \left(\frac{\partial I}{\partial t} + u \frac{\partial I}{\partial r} + v \frac{\partial I}{\partial z} \right) + p \left(\frac{\partial (ru)}{r \partial r} + \frac{\partial v}{\partial z} \right) = 0 \tag{4}$$

Equation of State

$$p = p\ (\rho, I) \tag{5}$$

where,

ρ = density (gm/cm^3).

u = radial velocity component (cm/sec).

v = axial velocity component (cm/sec).

r = radial coordinate (cm).

z = axial coordinate (cm).

p = pressure ($dynes/cm^2$).

I = specific internal energy (ergs/gm).

t = time (sec).

The conservation of mass is automatically satisfied by SHELLTC by neither allowing the creation nor destruction of mass. Mass which leaves one cell enters another and is accordingly added to the receiver cell and subtracted from the donor cell.

The axisymmetric grid used by SHELLTC is shown in Figure 1.

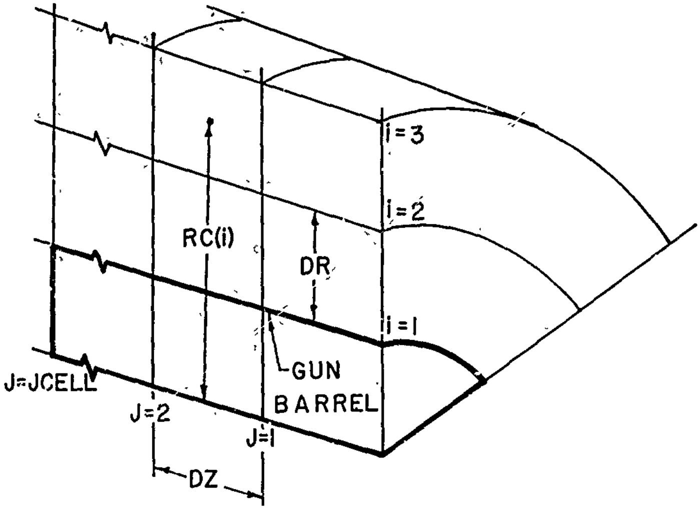

FIGURE 1

RC(i) is the radial distance to the center of cell in the i^{th} column. DR and DZ are the radial and axial dimensions of each cell, respectively. The cross-sectional area of each cell in the i^{th} column is given by,

$$TAU(I) = 2 \cdot \pi \cdot RC(i) \cdot DR \tag{6}$$

and its volume by,

$$VOL(I) = 2 \cdot \pi \cdot RC(i) \cdot DR \cdot DZ. \tag{7}$$

The conservation equations of momentum and energy are handled in two phases by SHELLTC. The first phase considers the fluid at rest and determines only the contributions of the pressure terms to the time derivative. The second phase of calculations accounts for mass transport. The finite difference equations used in SHELLTC are discussed in Appendix A along with the time increment calculations and the stability of SHELLTC.

INITIAL AND BOUNDARY CONDITIONS

A starting code, CLAMTC, is used to set up the grid used by SHELLTC and to initialize the fluid properties in each cell. The cell size chosen to simulate the 5"/54 gun blast was DZ = 5.0 inches (12.7 cm) and DR = 2.5 inches (6.35 cm). This allowed the radius of the gun barrel to be one cell and the length of the gun tube to be 54 cells. All fluid properties in each cell were initially set to ambient conditions by CLAMTC including the interior cells of the gun tube.

All boundary conditions and the interior ballistics at ejection were set at cycle 1 in SHELLTC. The left boundary of the grid (see Figure A-1, Appendix A) corresponding to the centerline of the gun barrel was set as reflective.* All other boundaries of the grid were set as transmissive** to allow flow out of the grid through these boundaries. The boundary of cells corresponding to I = 1 from $1 \leq J \leq 54$ was set reflective to simulate the gun barrel.

The initial fluid properties of the gas in the gun barrel at time of ejection of the projectile were obtained from interior ballistics data from the 5"/54 gun and some theoretical data. The muzzle pressure at ejection was assumed to be 8000 psi (5.52×10^8 dynes/cm^2). This value corresponds with experimental measurements [reference (9)] of muzzle pressure at ejection for the 5"/54, MARK 41 projectile. The variation of pressure along the gun tube was obtained from reference (12). The formula for p(x) is:

$$p(x) = \frac{12\, RT_o}{g\left(\frac{V_t}{W_c} - \eta\right)} \left[1.0 + \frac{W_c}{6W_p}\left(1.0 - \frac{3A^2x^2}{V_t^2}\right)\right] \qquad (8)$$

---

* A reflective boundary is one along which the normal component of the flow velocity is zero, the pressure gradient across the boundary is zero and there is no flux of the conserved quantities across the boundary.

** A transmissive boundary is a fictitious boundary across which flux of the conserved quantities is allowed without influence from points beyond the boundary.

where,

p = pressure at any point along bore, lb/in^2,

T_o = average temperature of gas at projectile ejection, ^oR,

R = gas constant, $ft\text{-}lb/lb/^oR$,

W_c = weight of propellant, lb.

W_p = weight of projectile, lb,

g = acceleration of gravity, ft/sec^2,

η = covolume, in^3/lb,

A = bore area, in^2,

V_t = total volume of bore and chamber, in^3

x = distance from breech, in.

Substitution of the above quantities for the 5"/54 gun into equation (8) gives a muzzle pressure of about 9000 psi. The specific impetus at ejection, RT_o, was therefore adjusted to yield a muzzle pressure corresponding to experimental data. The pressure at any position along the bore is then given by

$$p(x) = 9516 - .0208x^2. \quad (9)$$

The gas velocity was assumed to vary linearly from zero at the breech to 3000 ft/sec (9.144×10^6 cm/sec) at the muzzle at time of ejection. The gas temperature was assumed uniform along the length of the barrel and equal to 1526°K, which agrees with experimental data for the 5"/54 gun.

As noted earlier, a one material version of SHELL was used. The one material restraint does not allow for the distinction between propellant gases and ambient air. Thus the calculations are restricted to a single equation of state. The ideal gas equation of state with the ratio of specific heats of 1.4 was chosen for the first trial calculations. With these assumptions, the mass, density and specific internal energy of each of the cells comprising the gas inside the gun barrel are calculated by SHELLTC.

After the initial conditions at projectile ejection have been set, the flow both in the barrel and external to the barrel is determined only by the governing hydrodynamic equations and boundary conditions. Thus both the flow external and internal of the barrel is calculated.

RESULTS AND COMPARISON WITH EXPERIMENTAL DATA

The numerical calculations to simulate the gun blast from a 5"/54 gun were carried out using the digital CDC 6700 computer located at NWL. Calculations were carried out to 6.63 milliseconds after projectile ejection, requiring approximately 1.5 hours of computation time on the CDC 6700. The fluid properties of each cell were stored on magnetic tape every 3rd cycle (approximately every 0.075 milliseconds simulated time) for later analysis and plotting. The results of the calculations will be presented in this section and compared with experimental 5"/54 gun blast data.

The propagation of the calculated gun blast shock at 26.9° and 90° from the line of fire is shown in Appendix B, Figures B-1 and B-2, respectively. The shock fronts are smeared over 3 to 4 cells in both figures due to the artificial dissipation in SHELLTC. Note that in Figure B-1, the decaying pressure behind the shock deviates from nearly exponential at 1.3 milliseconds (cycle 62), giving the appearance of an inward facing second shock. This is the initial appearance of the normal shock at the leading edge of the shock bottle. At about 5.0 milliseconds (cycle 210) the normal shock has become stationary and the pressure signature behind the shock front is approaching its expected shape. The normal shock of the shock bottle appears stationary at 6 feet from the muzzle or about 14.4 calibers. Experimental measurements [reference (12)] indicate that the shock bottle becomes stationary at about 15 calibers from the muzzle. The oblique shock bounding the shock bottle near the muzzle can be seen in Figure B-2 and appears about one foot from the muzzle. Thus the hydrodynamic code appears to predict both the formation and location of the normal shock at the front edge of the shock bottle and the oblique shock bounding the shock bottle.

To compare the theoretical calculations with the existing experimental data, particular locations about the muzzle were chosen and the calculated pressure plotted as a function of time. Figure B-3 shows the resulting calculated pressure-time history at 5 feet from the muzzle and 90° from the line of fire. Figure B-4 shows the experimentally measured overpressure [reference (13)] at the same location. The calculated peak overpressure is about 13.4 psi and the positive duration is 1.32 milliseconds.

In measuring the duration, the rise time of the shock front was not included. The experimental peak overpressure is about 12.8 psi and the duration is 1.30 milliseconds. Calculated and experimental pressure traces at 5 feet from the muzzle and 135° from the line of fire are plotted as Figure B-5 and B-6, respectively. The calculated peak overpressure is about 3.3 psi as compared to 3.1 psi experimentally, and the calculated duration is 0.93 milliseconds as compared to 1.07 milliseconds measured experimentally.

Figures B-7 through B-13 show the velocity vectors predicted by SHELLTC at 1.25, 2.0, 2.5, 3.0, 3.5 and 4.5 milliseconds after projectile ejection, respectively. These CALCOMP plots were generated by SHPLOT, a plotting code developed for use with SHELLTC. Both the normal and oblique shocks of the shock bottle are clearly distinguishable after 2.5 milliseconds (Figure B-9). The absence of velocity vectors in some regions behind the gun is because velocities less than 328 feet per second (1.0 x 10^4 cm/sec) are not plotted. This was done because the size of the vector was as small as the arrow and the vector magnitudes could not be distinguished in these regions.

Qualitatively, three interesting phenomenon may be observed in Figures B-7 through B-13. First, the boundaries of the shock bottle are easily discernible in these figures, showing both the normal and oblique shocks described earlier. Second, the shock front is shown, and also its propagation with time. Third, a circulating flow "smoke ring" is shown which is observed in many gun firings.

Quantitatively, few if any velocity measurements of the gas outside the gun barrel have been made. Thus, no experimental data exists to compare with the calculated velocity field. The calculations do, however, predict the observed phenomena discussed above.

Figures B-14 and B-15 show the calculated and experimentally measured shock front positions, respectively, as a function of time. The calculated shock is seen to be somewhat slower than the actual shock, particularly aft of the muzzle. The general difference in shock velocity may be attributed to the simple equation of state used in SHELLTC and the limitation to one material. The larger difference aft of the muzzle may be due to the absence of the effects of the projectile on the shock. T. D. Taylor reference (14) has numerically solved the inviscid flow equations and calculated the muzzle blast for a 4.2 inch mortar with and without a shell in the flow. His results indicate a stronger blast field aft of the muzzle with a shell than without and thus a larger shock velocity behind the muzzle. However, no comparisons are made with experimental data in reference (14).

The stability of SHELLTC is discussed in Appendix A. The energy dissipating parameters S1, S2 and S3 (see Appendix A) were all set to zero for the calculations presented in this report. Thus the only dissipation effects were those inherent in SHELLTC. Close examination of Figure B-10 shows that one velocity vector near the axis of symmetry is negative. This is a result of an instability which occurred at about cycle 125 and can be seen to grow with time from Figures B-11 through B-13. The instability appears to grow as a disturbance in the flow. It did not effect the shock front, at least out to cycle 260, which was of primary interest in these calculations. No attempt was made to resolve the instability because of the lengthy running time on the computer. However, variation of the energy dissipating parameters to increase the artificial dissipation may resolve the instability.

CONCLUSIONS AND PLANS FOR FUTURE WORK

The two dimensional hydrodynamic code, SHELLTC, has been shown suitable for the calculation of a free-air muzzle blast. Reasonably good agreement was obtained between calculated and experimental values of peak overpressure and duration at several locations about the muzzle. The initial conditions in the barrel at projectile ejection were obtained from experimental measurements and interior ballistics theory. Because the full length of the gun barrel was simulated by the grid, no assumptions were necessary as to the variation with time of the fluid properties in the gun barrel.

The actual cost of computer time to simulate the 5"/54 gun blast presented in this report was about $1200 on the CDC 6700 computer. This cost is not unreasonable compared to firing one round from the 5"/54 gun. To obtain similar information experimentally would require multiple channels of instrumentation and still would not produce but a small portion of the data obtained from the calculations. The finite difference calculations easily allow the variation of parameters such as muzzle pressure, gas velocity, thermal energy and barrel length, to determine their effects on the gun blast field. Also, the computer provides data on the velocity field, which cannot be obtained using conventional instrumentation.

Additional calculations using a multi-material version of SHELL are planned. These calculations will include more precise equations of state for each material and allow chemical reactions to occur between materials. These calculations should predict the free-air blast field more precisely and give further insight of the shock bottle and secondary blast, due to muzzle flash.

There are many applications for the predicted gun blast field. In addition to gaining insight to the blast phenomena, propellant gas influences on the projectile outside the muzzle may now be calculated. The predicted blast field presented in this report has already been used to predict the effects of the propellant gas on the motion of fragments of a rotating band which has been torn from a projectile at ejection from the muzzle.

REFERENCES

1. Walther, M. F., "Gun Blast From a 5"/54 Gun," Report No. 1608, U.S. Naval Proving Ground, July, 1958.

2. Dodson, T. I. and Folk, T. L., "Free-Air Blast From 3"/50 Caliber Gun," Report TR-2222, U.S. Naval Weapons Lab., Oct., 1968.

3. Ingham, R. W., "Calculation of Gun Blast Loading on Ship Structure," Code 442 Memo ALNAV 59-53, BuShips, 1952.

4. Walther, M. F., "Gun Blast From Naval Guns," Report TR-2733, U.S. Naval Weapons Lab., Aug., 1972.

5. Nawrocki, E. A., et al., "Theoretical Calculations of the Phenomenology of the Distant Plain Event 6," AFWL TR-67-57, Air Force Weapons Lab., Kirtland AFB, New Mexico, 1967.

6. Needham, C. E., et al., "Theoretical Calculations of the Detonation of a 1000 Pound Sphere of TNT at 15 Feet Above Ground Level," AFWL TR-66-128, Air Force Weapons Lab., Kirtland AFB, New Mexico, 1966.

7. Needham, C. E., and Burghard, T., "Air Blast Calculation, Event MINE UNDER," AFWL TR-69-105, Air Force Weapons Lab., Kirtland AFB, New Mexico, 1969.

8. Leigh, G. G., "A Calculation of the Blast Wave from the Constant Velocity Detonation of an Explosive Sheet," PhD Thesis, Arizona State University, Tempe, Ariz., Sept., 1971.

9. Obrasky, J. S., Private Communication, Mechanical Design Branch, Engineering Department, Naval Weapons Laboratory, Dahlgren, Virginia, Dec. 1971.

10. Von Neumann, J. and Richtmeyer, R. D., "A Method for the Numerical Calculation of Hydrodynamic Shocks," Journal of Applied Physics, Vol. 21, p. 232, March 1950.

11. Harlow, F. H., "The Particle-in-cell Computing Method for Fluid Dynamics," Methods in Computational Physics, Vol. 3, p. 319, Academic Press, New York, 1964.

12. Engineering Design Handbook, Gun Series, "Muzzle Devices," U.S. Army Material Command, AMCP 706-251, May, 1968.

13. Soo Hoo, G. and Yagla, J. J., "Use of a Conical Muzzle Device to Control Gun Blast," Report TR-2793, U.S. Naval Weapons Lab., Aug., 1972.

14. Taylor, T. D., "Calculation of Muzzle Blast Flcw Fields," Northrop Corporate Lab., for Feltman Research Lab., Picatinny Arsenal, Dover, New Jersey, Contact No. DAAG07-69-C-0739, Dec., 1970.

APPENDIX A

FINITE DIFFERENCE EQUATIONS OF SHELLTC

The conservation equations are handled in two phases by SHELLTC. The first phase considers the fluid at rest and determines only the contributions of the pressure terms to the time derivative. Dropping the transport terms in the momentum and energy equations see equations (2), (3) and (4) , they become, in finite difference form, the following:

Momentum

$$U_K = U_K^{(n)} + \frac{1}{\rho^{(n)}} \frac{PL^{(n)} - PR^{(n)}}{\Delta r} \Delta t \qquad \text{(A-1)}$$

$$V_K = V_K^{(n)} + \frac{1}{\rho^{(n)}} \frac{PB^{(n)} - PT^{(n)}}{\Delta z} \Delta t \qquad \text{(A-2)}$$

Energy

$$I_K = I_K^{(n)} + \frac{P_K^{(n)}}{\rho_K^{(n)}} \left[\frac{\tilde{VB}^{(n)} - \tilde{VT}^{(n)} + \tilde{VB} - VT}{\Delta z} \right.$$

$$\left. + \frac{2}{r_i + r_{i-1}} \frac{UL^{(n)} - UR^{(n)} + \tilde{UL} - \tilde{UR}}{\Delta r} \right] \frac{\Delta t}{2} \qquad \text{(A-3)}$$

where

$$PL = \frac{P_K + P_{KL}}{2} \qquad PR = \frac{P_K + P_{KR}}{2}$$

$$PB = \frac{P_K + P_{KB}}{2} \qquad PT = \frac{P_K + P_{KT}}{2}$$

$$VB = \frac{V_K + V_{KB}}{2} \qquad VT = \frac{V_K + V_{KT}}{2}$$

$$UL = \frac{u_K(r_i + r_{i-1}) + u_{KL}(r_{i-1} + r_{i-2})}{4}$$

$$UR = u_K(r_i + r_{i-1}) + u_{KL}(r_{i+1} + r_i)$$

K is the index of the cell center and i is the index of the right-hand boundary of the K^{th} cell. The adjacent cells to the K^{th} cell are identified in Figure A-1.

Two successive passes are made through the first phase of calculations of each cell. New velocities are calculated from the momentum equations for a full time step. The internal energy is calculated for a half time step using the old velocities. The internal energy is then calculated for the remaining half time step using the new velocities. After each pass through phase one, the internal energy of the cell is checked to insure that it has not become negative. Should such an event occur, a negative time step is used to return the state of the fluid to its original state at the beginning of the cycle and a smaller time step is calculated.

The second phase of calculations accounts for mass transport. The equation for conservation of mass [equation (1)] becomes, in finite difference form,

$$\frac{\Delta\rho}{\Delta t} = \left[\frac{r_{i-1}\,\rho_{i-1}\,u_{i-1}}{r_{i-\frac{1}{2}}\,\Delta r} - \frac{r_i\,\rho_i\,u_i}{r_{i-\frac{1}{2}}\,\Delta r} + \frac{\rho_{j-1}\,v_{j-1} - \rho_j v_j}{\Delta z} \right] \qquad \text{(A-4)}$$

The conservation of mass equation can be written in another form as

$$M_k^{(n+1)} = M_k^{(n)} + \Pi\Delta t \left[(r_i^2 - r_{i-1}^2)(\bar{v}_B\rho_B - \bar{v}_T\rho_T) + 2\Delta z\,(r_{i-1}\,\bar{u}_L\rho_L - r_i\,\bar{u}_R\rho_R) \right] \qquad \text{(A-5)}$$

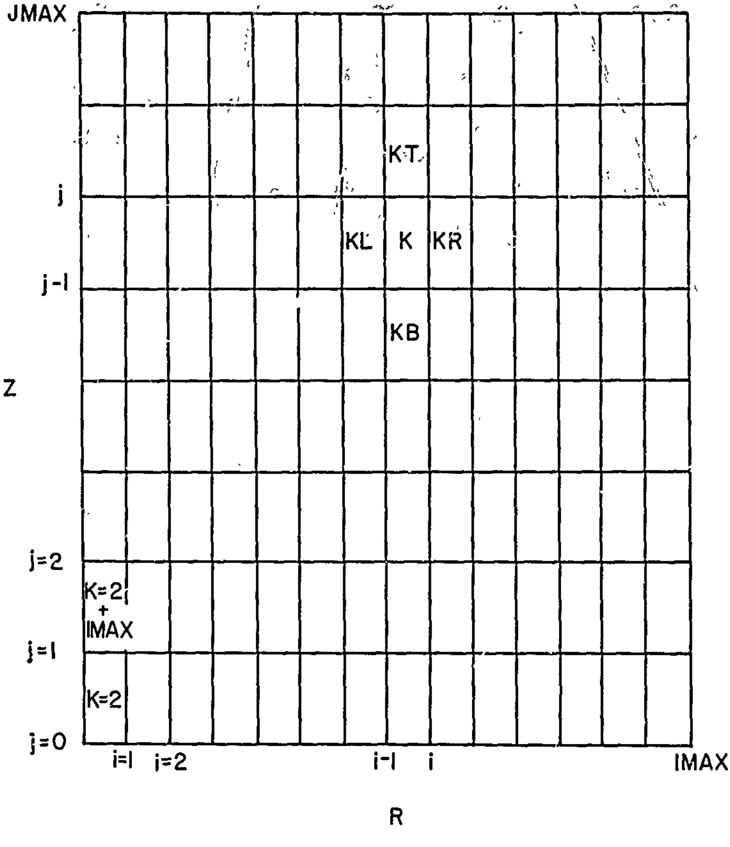

FIGURE A-1 SHELLTC Mesh

where $\overline{v\rho}$ is the mass flux across a face of cell k and the subscripts B, T, L and R designate bottom, top, left and right faces, respectively. The densities are those of the donor cells and the velocities are given by:

$$\bar{v} = \frac{1/2\ (v_T + v_K)}{1 + (v_R - v_K)\frac{\Delta t}{\Delta z}}$$

$$\bar{u} = \frac{1/2\ (u_R + u_K)}{1 + (u_R - u_K)\frac{\Delta t}{\Delta z}} \qquad \text{(A-6)}$$

This velocity weighting scheme is used to ensure stability in regions behind a shock front.

Calculation of the mesh cells by SHELLTC proceeds from bottom to top and from left to right. Thus mass transport for each cell is calculated for the top and right faces only. The new mass in the K^{th} is given by

$$M_K^{(n+1)} = M_K^{(n)} + \Delta M_B + \Delta M_L - \Delta M_T - \Delta M_R \qquad \text{(A-7)}$$

where the ΔM's are the masses transported across the respective faces of the K^{tn} cell.

New velocities are computed using the conservation equations for axial and radial momentum as follows:

$$v_K^{(n+1)} = \frac{M_K^{(n)}\ v_K + \Delta M_B v_B + \Delta M_L v_L - \Delta M_T\ v_T - \Delta M_R v_R}{M^{(n+1)}} \qquad \text{(A-8)}$$

The new specific internal energy is computed by adding the total energy carried by the transported masses to the k^{th} cell minus the new kinetic energy and then dividing by the new mass.

$$I_K^{(n+1)} = \Big(M_K^{(n)} \left[I_K + \tfrac{1}{2} (u_K^2 + v_K^2) \right] + \Delta M_B \left[I_B + \tfrac{1}{2} (u_B^2 + v_B^2) \right]$$

$$+ \Delta M_L \left[I_L + \tfrac{1}{2} (u_L^2 + v_L^2) \right] - \Delta M_T \left[I_T + \tfrac{1}{2} (u_T^2 - v_T^2) \right]$$

$$- \Delta M_R \left[I_R + \tfrac{1}{2} (u_R^2 + v_R^2) \right] \Big) \Big/$$

$$\left(M_K^{(n+1)} - \frac{\tfrac{1}{2} \left[u^{(n+1)} \right]^2 - \tfrac{1}{2} \left[v^{(n+1)} \right]^2}{M^{(n+1)}} \right) \qquad \text{(A-10)}$$

The time step, Δt, is determined by consideration of stability to satisfy two conditions. First, the Courant condition which prohibits the transmission of a signal across more than one cell in one time step. Second, that $|u/\Delta r|_{max}$ and $|v/\Delta z|_{max}$ be less than $1/\Delta t$, thus prohibiting the transport of mass across more than one cell in one time step.

STABILITY

Von Neumann and Richtmeyer, reference (10), have shown that the hydrodynamic equations can be solved numerically if an artificial dissipation term is introduced. This in effect smears the shock front making the fluid properties such as pressure, density, entropy and internal energy continuous across the shock. Thus the Rankine-Hugoniot conditions are satisfied across the shock and the numerical calculations proceed as if no shock were present.

The first phase of SHELLTC calculations are unstable, because they contain no dissipative mechanism. However, the second phase, which deals with the mass movement, has been shown by Harlow, reference (11), to give stability to the calculations by adding effective viscosity and effective heat conduction.

In addition to the inherent dissipative effect in SHELLTC, Nawrocki, reference (5), has added an artificial viscosity scheme to SHELLTC. By appropriate selections of the three parameters S1, S2, and S3, the energy dissipating effect may be varied to enhance or diminish the inherent effective dissipation in SHELLTC.

Leigh, reference (8), has conducted a parametric study of a one-dimensional planar blast wave to determine the effect of variations in these parameters. His results are presented in reference (8). A listing of the basic SHELLTC code is also given in reference (8).

APPENDIX B

FIGURES

FIGURES

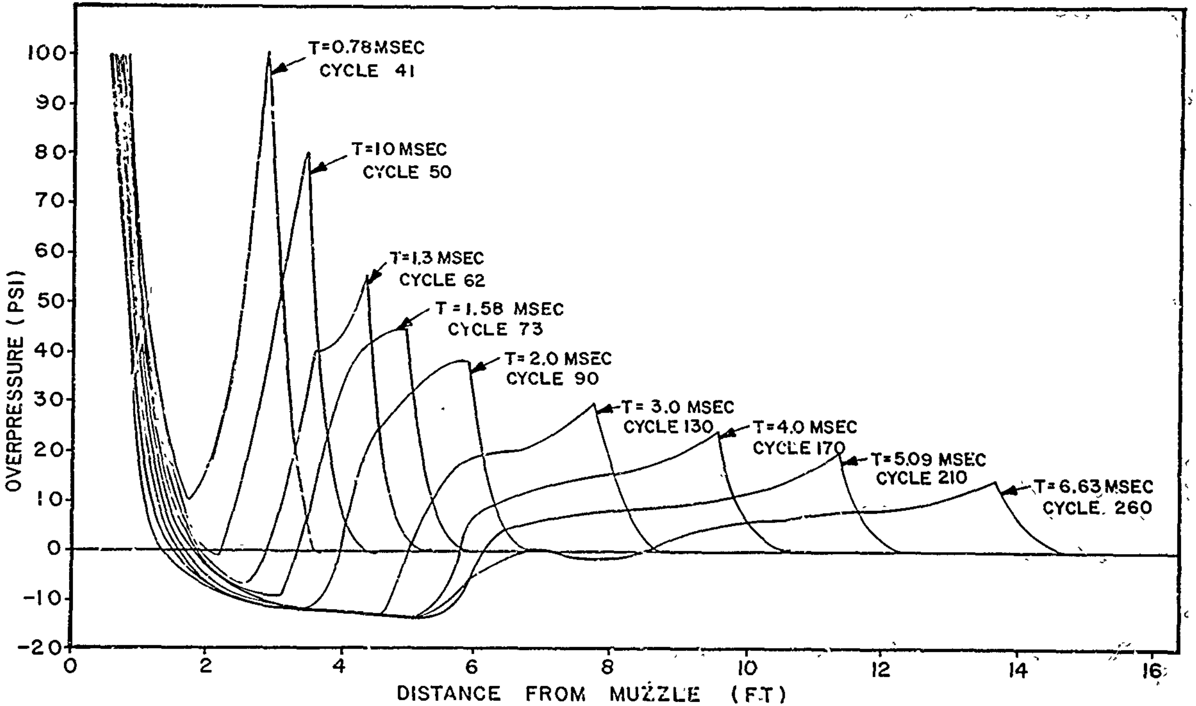

THEORETICAL GUN BLAST AT 26.9° FROM LINE OF FIRE

FIGURE B-1

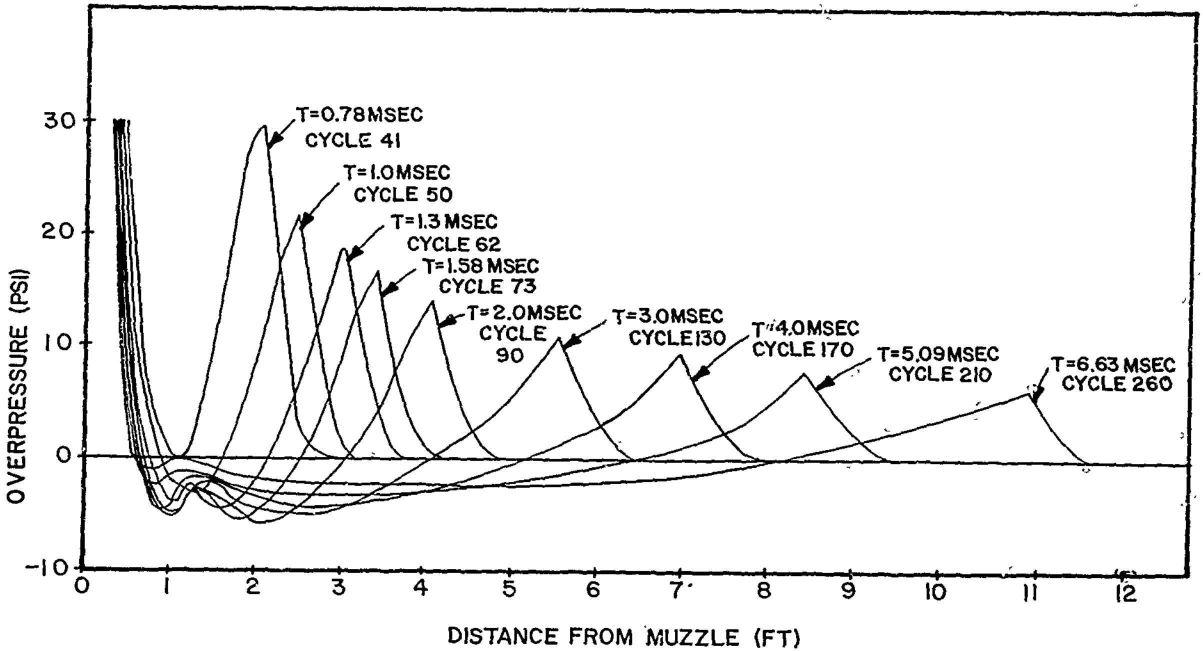

THEORETICAL GUN BLAST AT 90° FROM LINE OF FIRE

FIGURE B-2

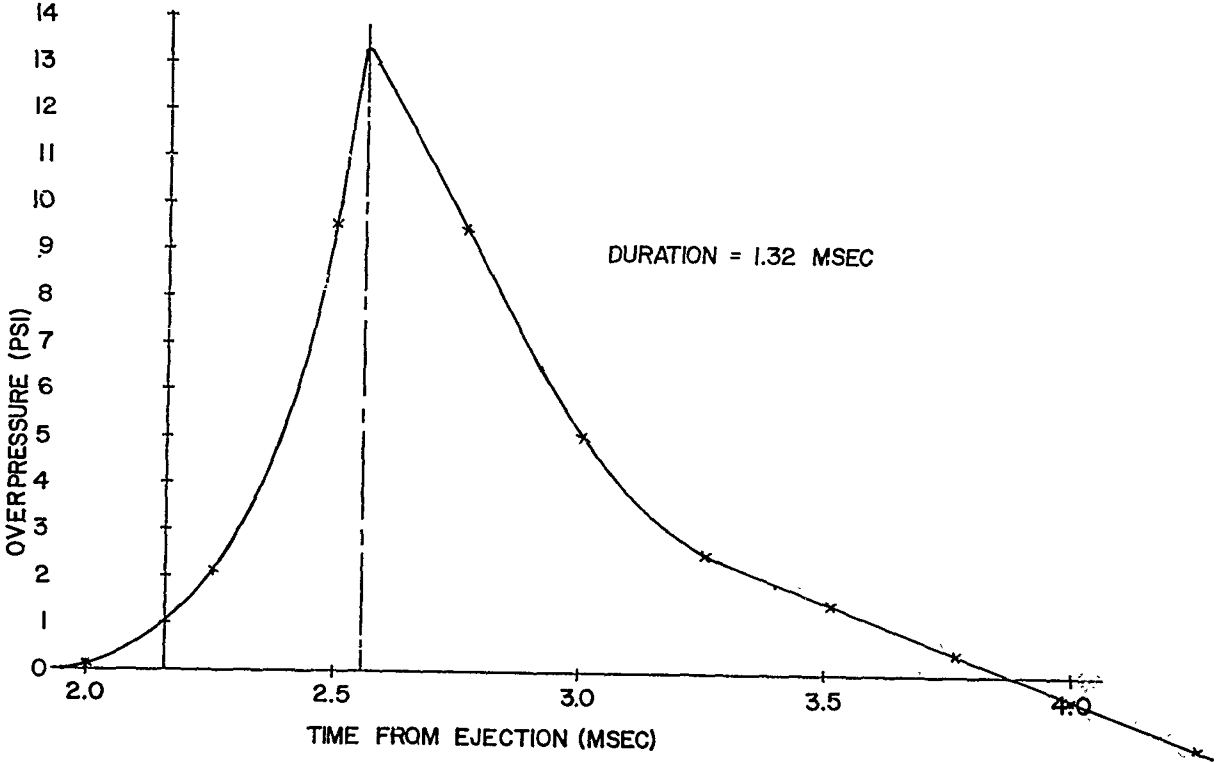

THEORETICAL 5"/54 GUN BLAST AT 5 FT. AND 90 DEGREES

FIGURE B-3

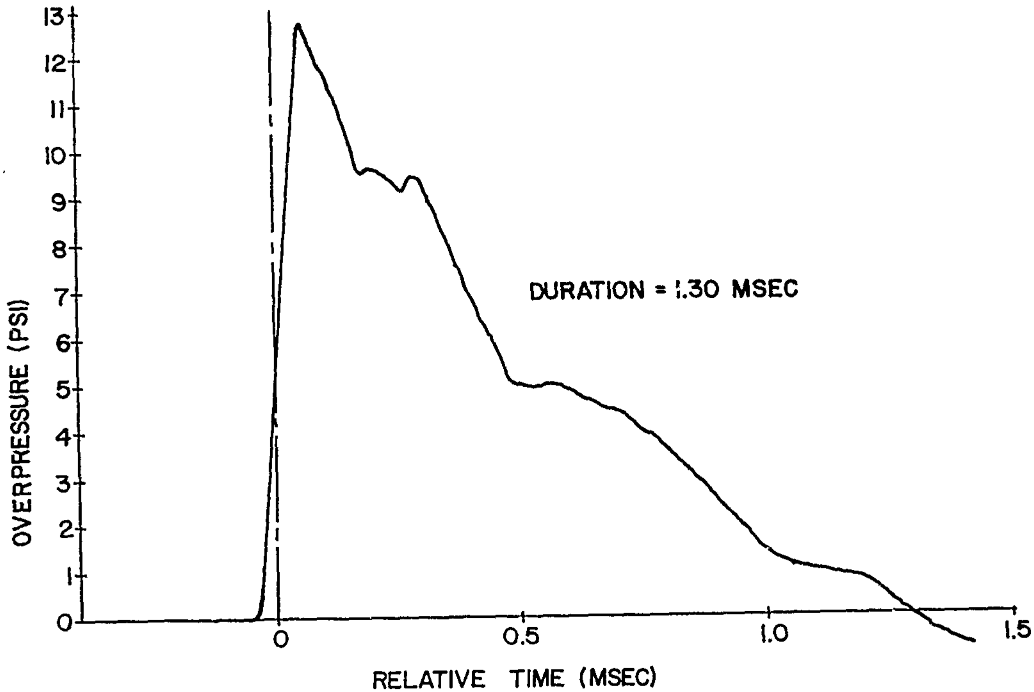

EXPERIMENTAL 5"/54 GUN BLAST AT 5FT. AND 90 DEGREES

FIGURE B-4

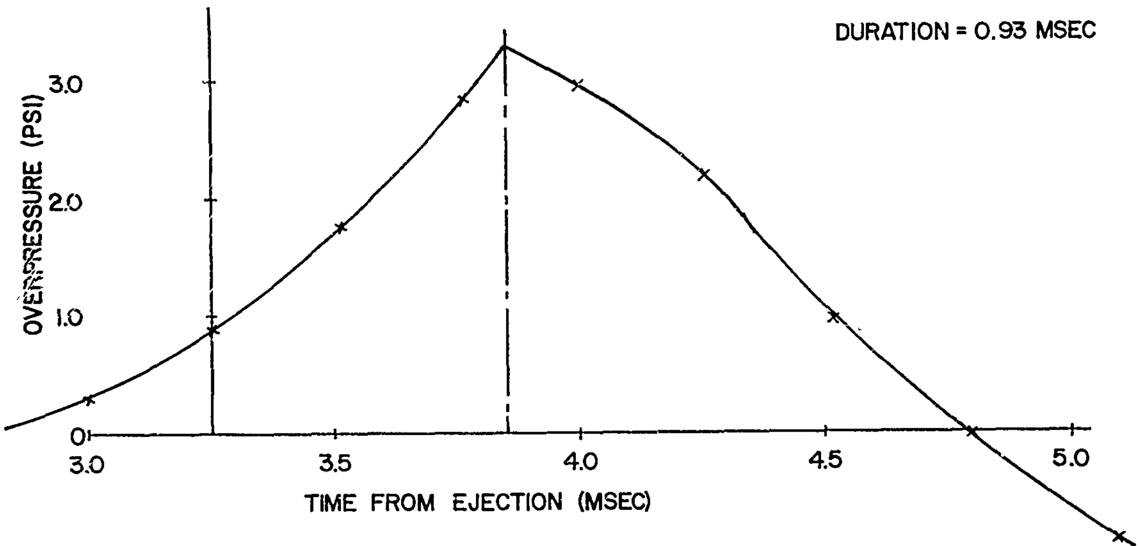

THEORETICAL 5"/54 GUN BLAST AT 5 FT. AND 135 DEGREES

FIGURE B-5

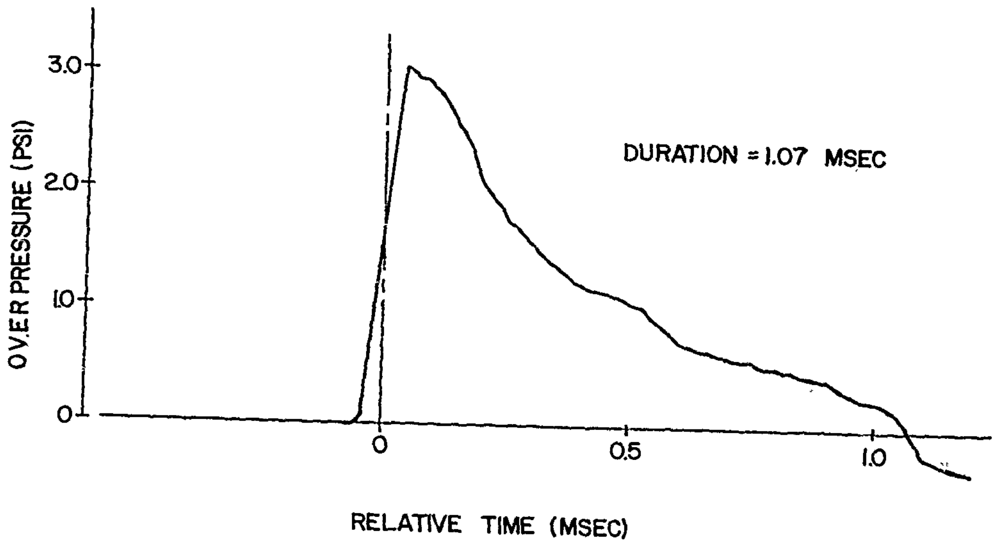

EXPERIMENTAL 5"/54 GUN BLAST AT 5 FT. AND 135 DEGREES

FIGURE B-6

VELOCITY VECTOR

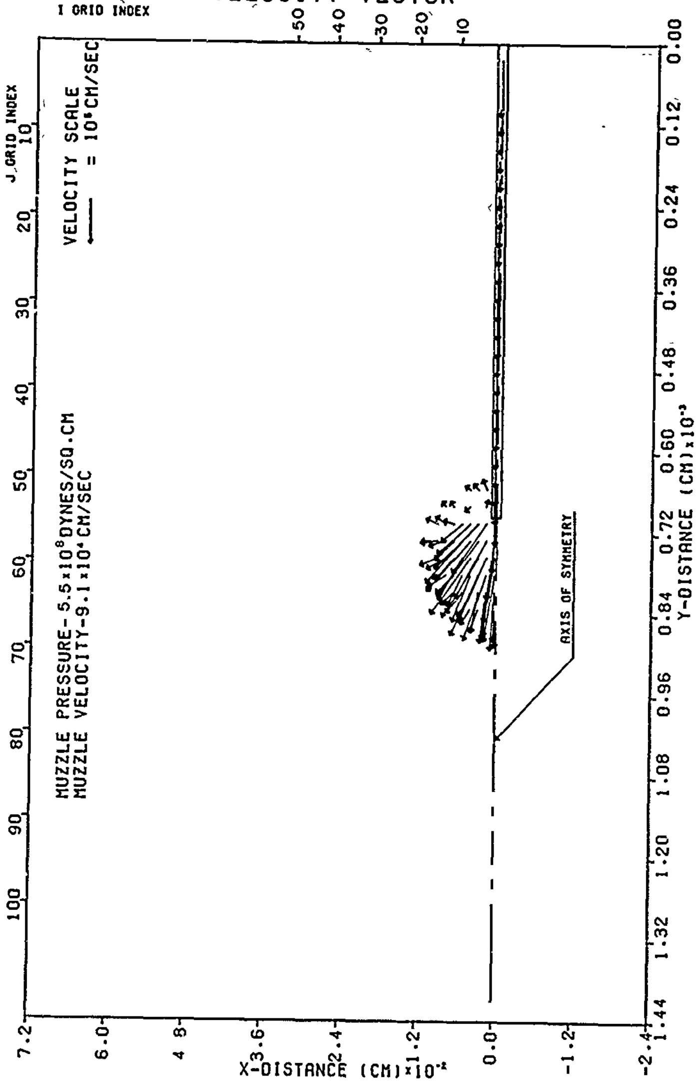

5 INCH /54 SIMULATED GUN BLAST (1/17/72)
TIME 0.001253 SEC CYCLE 60 PROBLEM 554
FIGURE B-7

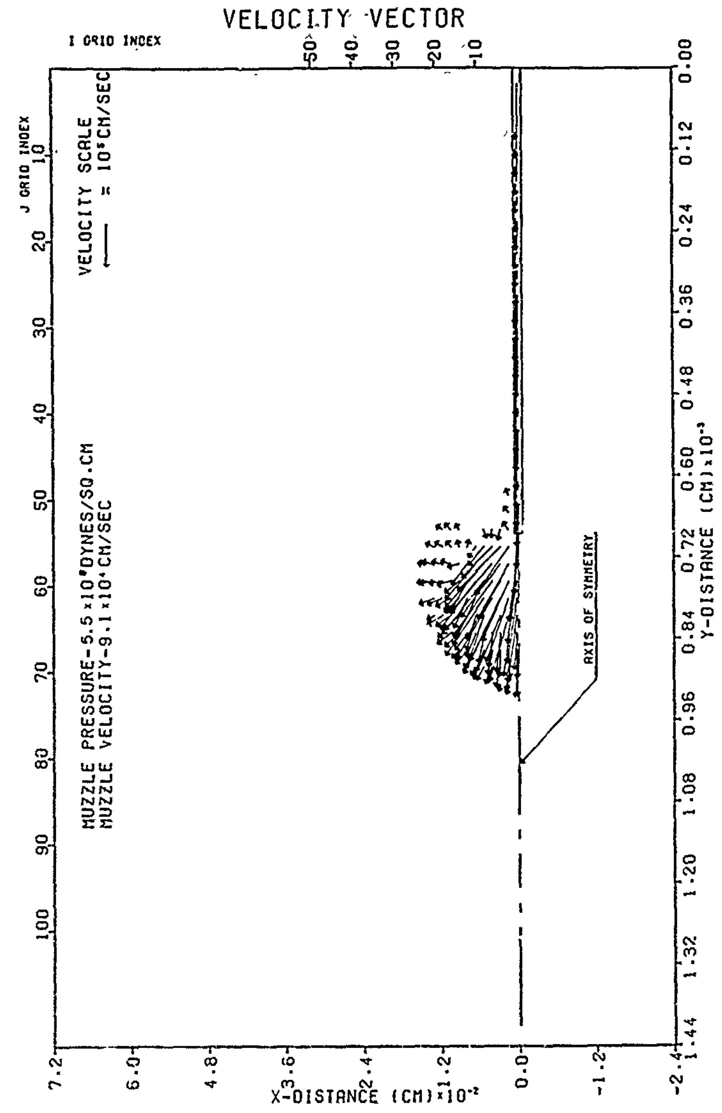

5 INCH /54 SIMULATED GUN BLAST (1/17/72)

TIME 0.002000 SEC   CYCLE 90   PROBLEM 554

FIGURE B-8

VELOCITY VECTOR

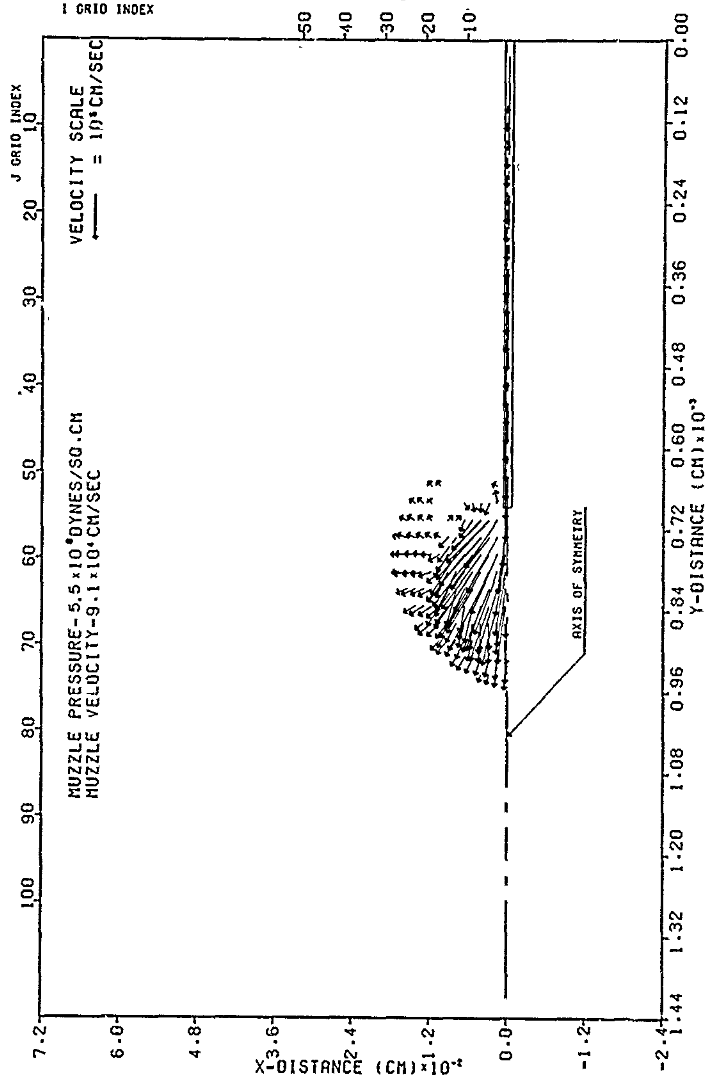

5 INCH /54 SIMULATED GUN BLAST (1/17/72)

TIME 0.002500 SEC CYCLE 110 PROBLEM 554

FIGURE B-9

VELOCITY VECTOR

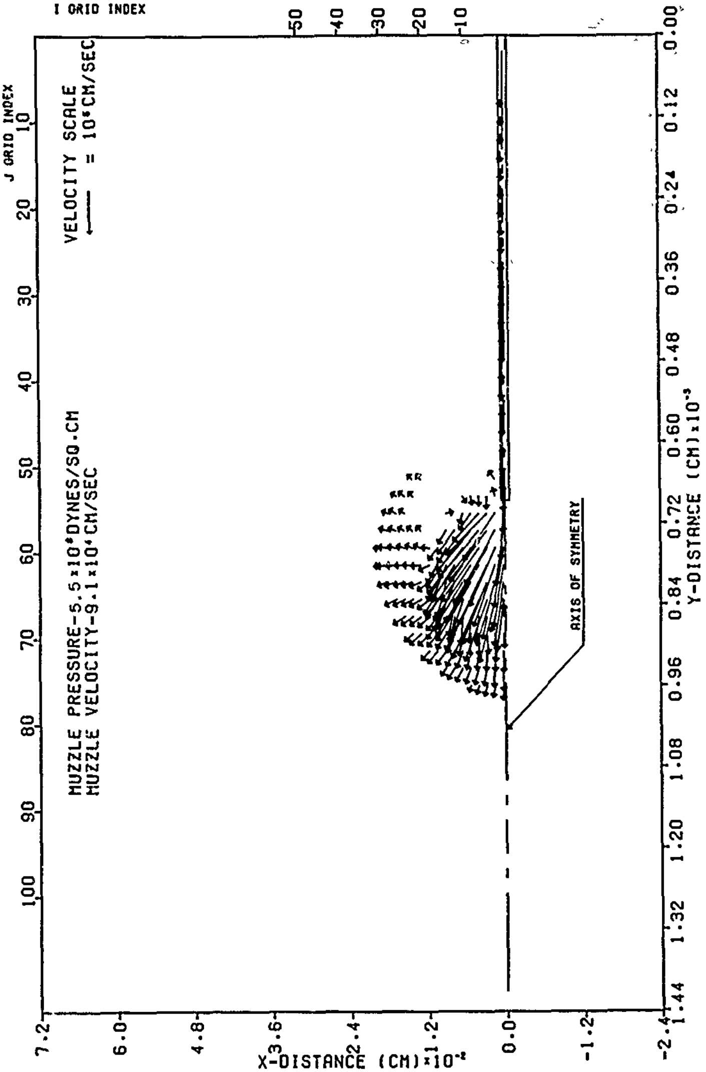

5 INCH /54 SIMULATED GUN BLAST (1/17/72)

TIME 0.003000 SEC CYCLE 130 PROBLEM 554

FIGURE B-10

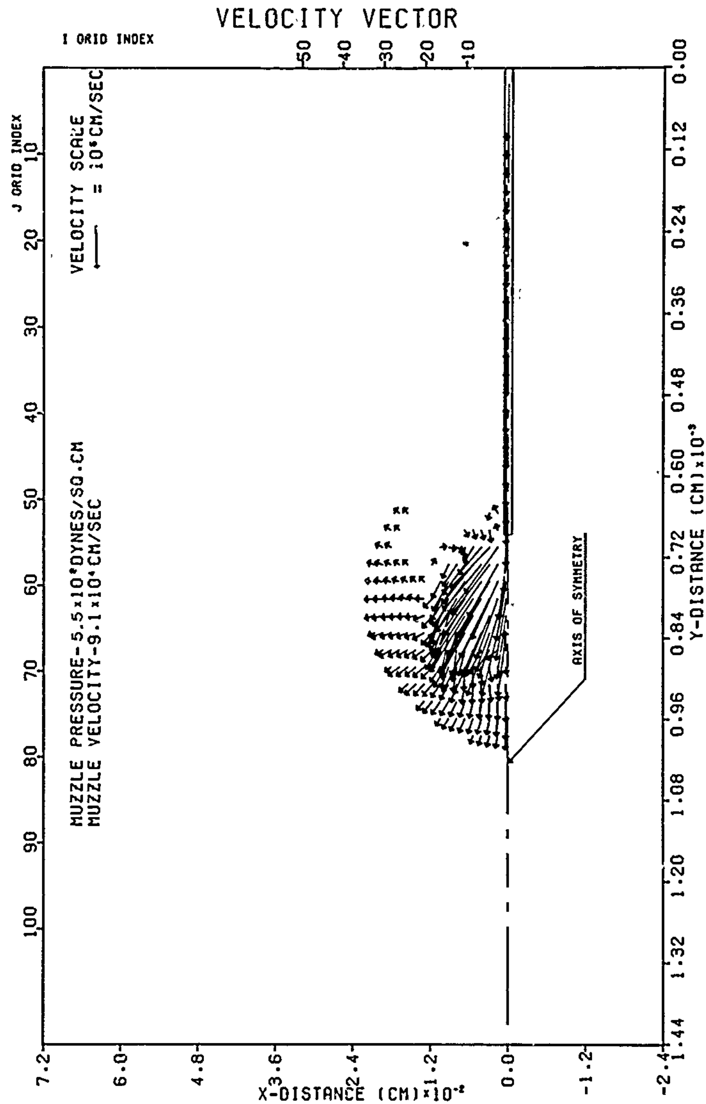

5 INCH /54 SIMULATED GUN BLAST (1/17/72)
TIME 0.003511 SEC CYCLE 150 PROBLEM 554

FIGURE B-11

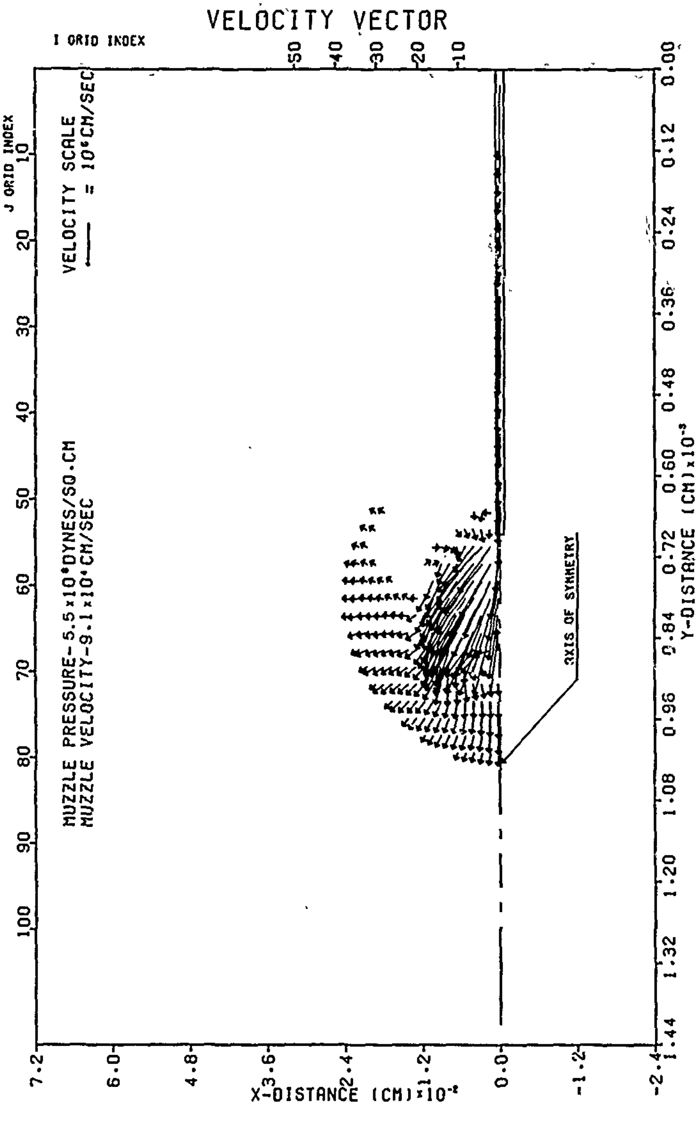

5 INCH /54 SIMULATED GUN BLAST (1/17/72)

TIME 0.004000 SEC CYCLE 170 PROBLEM 554

FIGURE B-12

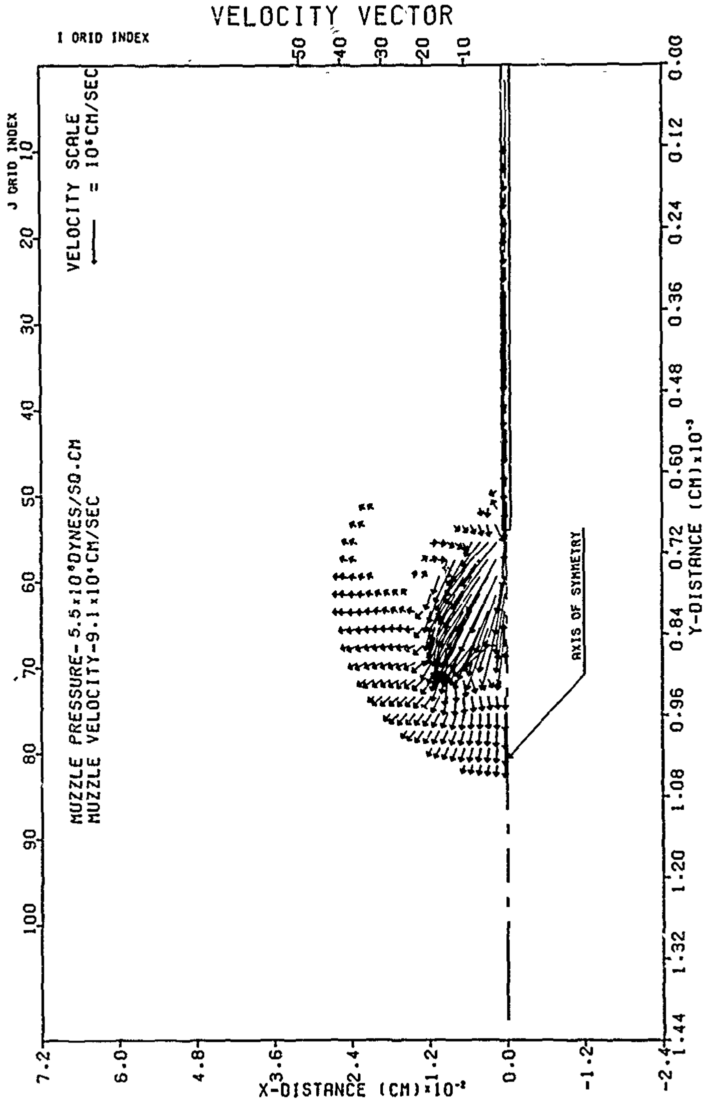

5 INCH /54 SIMULATED GUN BLAST (1/17/72)

TIME 0.004530 SEC CYCLE 190 PROBLEM 554

FIGURE B-13

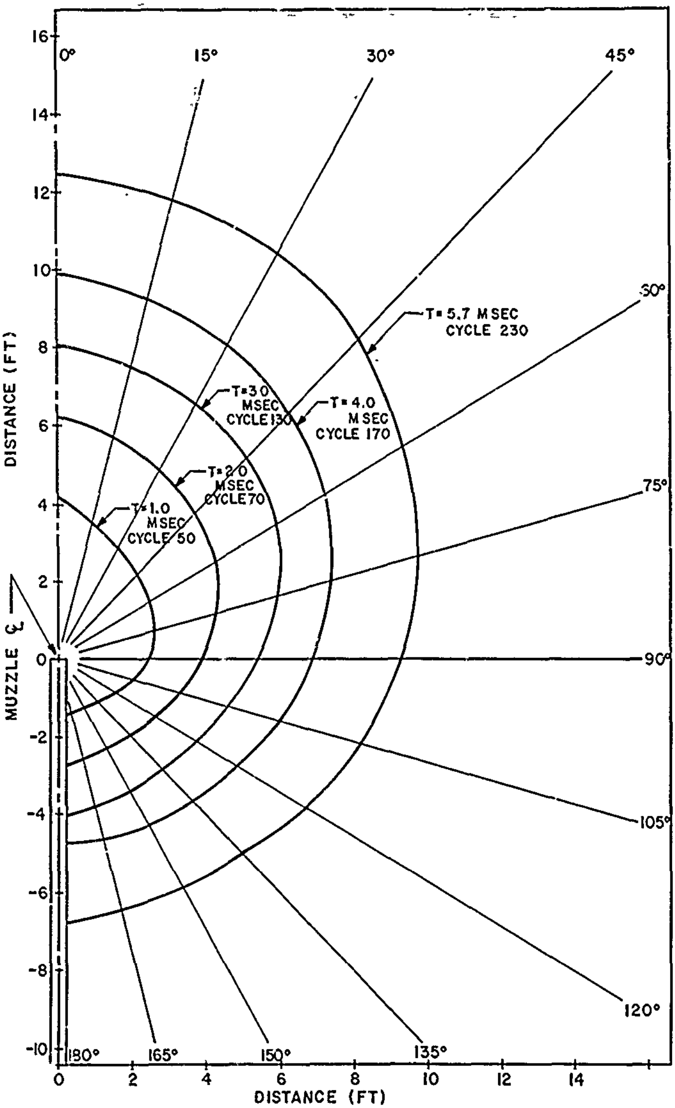

5"/54 THEORETICAL SHOCK ARRIVAL TIMES

FIGURE B-14

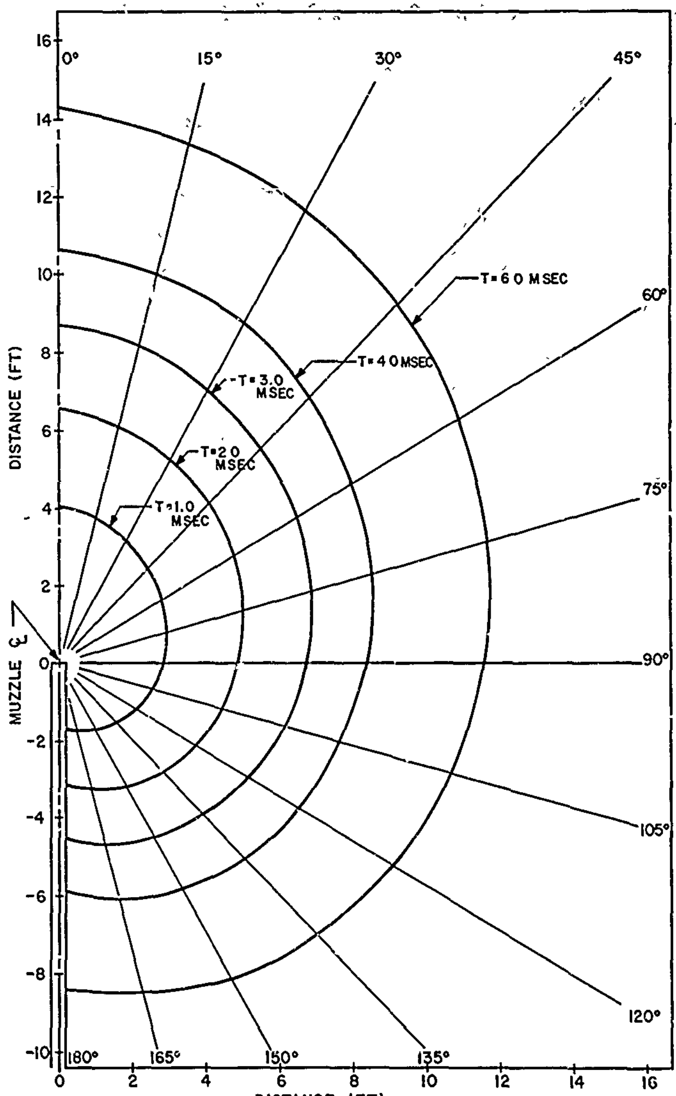

5"/54 EXPERIMENTAL SHOCK ARRIVAL TIMES

FIGURE B-15

APPENDIX C

DISTRIBUTION

DISTRIBUTION

Headquarters Naval Material Command
Director of Naval Laboratories Programs
Special Assistant Dr. J. H. Huth (Code NMAT03L4)
Crystal Plaza No. 6 (Room 980)
2221 Jefferson Davis Highway
Arlington, Virginia 20360

Naval Ordnance Systems Command
Washington, D. C. 20360

Attn: ORD 533	(4)
ORD 553	(4)
ORD 542	(4)
ORD RMO-403	

Naval Air Systems Command
Washington, D. C. 20360

Attn: AIR 530212	(8)

Naval Ship System Command
Washington, D. C. 20360

Attn: Code PMS 378.1B	(4)
Code 423	(4)

Naval Ships Engineering Center
Center Building Prince Georges Center
Hyattsville, Maryland 20982

Attn: SEC 6105	(4)
6128C	(4)
6140E	(4)
6161C	(4)

Commander
Naval Ordnance Laboratory/White Oak
Silver Spring, Maryland 20901

Attn: Joseph Pittman	(2)

Commanding General
Human Engineering Laboratory
Aberdeen Research and Development Center
Aberdeen, Maryland 21005

Attn: George Carinther	(1)

DISTRIBUTION

Commanding General
Ballistics Research Laboratory
Aberdeen, Maryland W 21005
Attn: Julius Meszaros (2)

Commanding General
Rock Island Arsenal
Rock Island, Illinois
Attn: Mark Salsbury (2)

Southwest Research Institute
San Antonio, Texas
Attn: P. S. Westine (2)

Applied Physics Laboratory
Johns Hopkins University
8621 Georgia Avenue
Silver Spring, Maryland
Attn: M. B. Tate (2)

Defense Documentation Center
Cameron Station
Alexandria, Virginia 22384 (2)

Local:
T
TM
TT
TA
TP
TI
TIE
TIER (20)
K
G
E
F
MIP (5)
MIL (2)
MIM

UNCLASSIFIED

Security Classification

DOCUMENT CONTROL DATA - R & D

(Security classification of title, body of abstract and indexing annotation must be entered when the overall report is classified)

1. ORIGINATING ACTIVITY *(Corporate author)* Naval Weapons Laboratory Dahlgren, Virginia 22448	2a. REPORT SECURITY CLASSIFICATION UNCLASSIFIED 2b. GROUP

3. REPORT TITLE

FINITE DIFFERENCE CALCULATIONS OF THE FREE-AIR GUN BLAST ABOUT THE MUZZLE OF A 5"/54 NAVAL GUN

4. DESCRIPTIVE NOTES *(Type of report and inclusive dates)*

5. AUTHOR(S) *(First name, middle initial, last name)*

Dr. G. R. Moore

6. REPORT DATE	7a. TOTAL NO. OF PAGES	7b. NO. OF REFS
September 1972		

8a. CONTRACT OR GRANT NO	9a. ORIGINATOR'S REPORT NUMBER(S)
b. PROJECT NO.	NWL TR-2794
c.	9b. OTHER REPORT NO(S) *(Any other numbers that may be assigned this report)*
d.	

10. DISTRIBUTION STATEMENT

Distribution limited to U.S. Gov't. agencies only; Test and Evaluation; September 1972. Other requests for this document must be referred to the Commander, Naval Weappons Laboratory, Dahlgren, Virginia 22448.

11. SUPPLEMENTARY NOTES	12. SPONSORING MILITARY ACTIVITY

13. ABSTRACT

A two-dimensional hydrodynamic code has been used to calculate the free-air blast field about the muzzle of a 5"/54 Naval gun. The calculated blast pressure wave as a function of time is presented along with the velocity field. Calculated overpressures and durations are compared with experimental data. The calculations predict the formation and location of the shock bottle and formation of the "smoke ring".